Available online at www.sciencedirect.com
ScienceDirect
Journal of Molecular Graphics and Modelling 25 (2007) 721–730
Journal of Molecular Graphics and Modelling
www.elsevier.com/locate/JMGM

Molecular modelling of the $GABA_A$ ion channel protein

Valérie Campagna-Slater [a], Donald F. Weaver [a,b,c,*]

[a] Department of Chemistry, Dalhousie University, Halifax, Nova Scotia, Canada B3H 4J3
[b] Department of Medicine, Dalhousie University, Halifax, Nova Scotia, Canada B3H 2Y9
[c] School of Biomedical Engineering, Dalhousie University, Halifax, Nova Scotia, Canada B3H 3J5

Received 10 March 2006; received in revised form 8 June 2006; accepted 12 June 2006
Available online 17 June 2006

Abstract

The $GABA_A$ ion channel protein is central to the mechanism of action of general anaesthetics and thus to the phenomenon of human consciousness. A molecular model of the $\alpha_1\beta_2\gamma_2$ γ-aminobutyric acid type-A ($GABA_A$) ligand-gated ion channel protein has been constructed. The cryo-electron microscopy structure of the nicotinic acetylcholine receptor (nAChR) from *Torpedo marmorata* and the X-ray crystal structure of the acetylcholine binding protein (AChBP) from *Lymnaea stagnalis* were used as starting templates for comparative modelling. Features of the modelling approach used in the development of this $GABA_A$ model include: (1) multiple sequence alignment of members of the Cys-loop superfamily; (2) the design and implementation of a quasi-*ab initio* loop modelling algorithm; (3) expansion of the transmembrane domain (TMD) ion pore to model the open-state of the $GABA_A$ channel; (4) hydrophobicity analysis of the TMD to refine the structure in regions involved in general anaesthetic binding. The final model of the $\alpha_1\beta_2\gamma_2$ $GABA_A$ protein agrees with available experimental data concerning general anaesthetics.

Keywords: γ-Aminobutyric acid (GABA); γ-Aminobutyric acid type-A receptor ($GABA_A$); Ligand-gated ion channels; Molecular modelling; Transmembrane domain; General anaesthetic

1. Introduction

Since the $GABA_A$ ion channel protein is central to the mechanism of action of general anaesthetics and thus to the phenomenon of human consciousness, there is a need to devise robust molecular models of this protein. The γ-aminobutyric acid type-A receptor ($GABA_A$) is a ligand-gated ion channel belonging to the Cys-loop superfamily, which also includes the nicotinic acetylcholine receptor (nAChR), the glycine receptor (GlyR), the serotonin type 3 receptor ($5\text{-}HT_3$) and the γ-aminobutyric acid type-C receptor ($GABA_C$) [1,2]. These ligand-gated ion channels, characterized by a pentameric structure and a conserved disulphide-bridge present in the extracellular domain of each subunit isoform, are involved in fast synaptic transmission in the central nervous system (CNS). The five subunits of the pentameric structure span the lipid membrane and are arranged around a central ion pore. Upon binding of a specific neurotransmitter, allosteric movements in the channel structure result in an opening of the ion pore, allowing either negatively (GlyR, $GABA_A$, $GABA_C$) or positively (nAChR, $5\text{-}HT_3$) charged ions to traverse the lipid bilayer [2–4].

Each of the five subunits is comprised of three regions with distinct folds. First, the N-terminal ligand-binding domain (LBD) is found on the extracellular side of the membrane and consists primarily of β-strands. It is denoted as the ligand-binding domain since it binds the endogenous neurotransmitters such as γ-aminobutyric acid ($GABA_A$) or acetylcholine (nAChR). Next, the transmembrane domain (TMD) spans the lipid bilayer and approximately 10 Å further on the extracellular side. The TMD has been shown to be constituted of a four α-helix bundle [5]; herein, the four α-helices forming the TMD will be denoted TM1, TM2, TM3 and TM4, according to their position in the primary sequence. TM1 and TM3 face the adjacent subunits as well as the lipid bilayer, while TM2 faces the lumen of the pore, and TM4 is buried in the membrane (Fig. 1). Finally, a long cytoplasmic loop links TM3 and TM4. The secondary structure of the cytoplasmic domain remains

* Corresponding author. Tel.: +1 902 494 7183; fax: +1 902 494 1310.
E-mail address: donald.weaver@dal.ca (D.F. Weaver).

1093-3263/$ – see front matter © 2006 Elsevier Inc. All rights reserved.
doi:10.1016/j.jmgm.2006.06.001

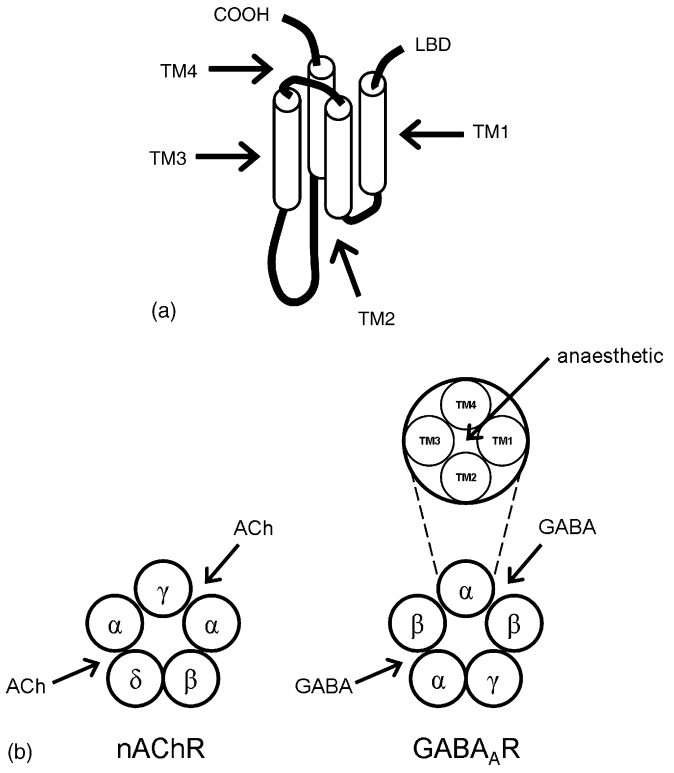

Fig. 1. (a) Relative position of the α-helices in the TMD of a subunit. (b) Subunit assemblies of the nAChR and $GABA_A$ receptor viewed from the extracellular side. The ACh, GABA, and anaesthetic binding sites are indicated by arrows.

uncertain, although it may contain a curved α-helix preceding TM4 [6]. The shorter loops linking TM1–TM2 and TM2–TM3 are included in the TMD.

GABA is a major inhibitory neurotransmitter. Upon binding of GABA to two binding sites situated at the β(+)/α(−) subunit interfaces within the $GABA_A$ protein, allosteric movements cause the channel to open, allowing for an influx of chloride ions into the neuron and causing hyperpolarization across the membrane. A variety of other molecules bind to the $GABA_A$ receptor, acting as agonists, antagonists, or modulators [7,8]. Minor tranquillizers of the benzodiazepine class bind as agonists at a site located at the α(+)/γ(−) subunit interface, and residues involved in benzodiazepine binding or action have been identified (see for example [9–13]). Other sedative-hypnotic molecules known to bind at various subtypes of the $GABA_A$ receptor include barbiturates and neurosteroids. Volatile anaesthetics, alcohols, and intravenous general anaesthetics such as etomidate and propofol act at sites located at the centre of the four α-helical segments composing the TMD. Several amino acids involved in $GABA_A$ modulation by general anaesthetics have been identified.

Nineteen $GABA_A$ subunit isoforms have been identified, namely $\alpha_{1–6}$, $\beta_{1–3}$, $\gamma_{1–3}$, $\rho_{1–3}$, δ, ε, θ and π. In the current study, the $\alpha_1\beta_2\gamma_2$ $GABA_A$ receptor is modelled, as it represents the most common subunit assembly in the human brain [2]; moreover, it has been demonstrated that the general anaesthetic etomidate has a GABA-modulatory effect only on the β_2 and β_3 subunit subtypes, but not on the β_1 subtype [14,15]. The purpose of this modelling study was to construct a robust computational model of the $\alpha_1\beta_2\gamma_2$ $GABA_A$ ion channel protein that satisfied known experimental data concerning general anaesthetic binding and function.

2. Methodology

2.1. Template selection

Template selection is an important starting point in comparative modelling, since it establishes a generalized folding model for the protein. Typically, a high quality experimentally determined structure is used as a template. Membrane-bound proteins however present a particular challenge for structural analysis through X-ray crystallography or spectroscopic techniques, as they rapidly become denatured upon extraction from their physiological lipid-membrane environment. These two standards for structural characterization are thus usually unable to resolve the structure of proteins such as the ligand-gated ion channels. Accordingly, there exist few well-resolved structures of membrane-bound proteins that can be used as templates for comparative modelling of the $GABA_A$ channel. However, developments have enabled the resolution of some membrane-bound proteins via cryo-electron microscopy. Although typical resolution for structural characterization by cryo-electron microscopy is lower than what can be obtained with the more traditional X-ray crystallography and NMR methods, it currently provides one of the only methods for structural resolution of some protein families.

The transmembrane section of the $GABA_A$ receptor was modelled using the cryo-electron microscopy structure of the nicotinic acetylcholine receptor (nAChR) of *Torpedo marmorata*, obtained at a 4 Å resolution (PDB entry 1OED) [5]. This structure provides a good starting template for the transmembrane portion of the $GABA_A$ receptor, given that the nAChR also belongs to the Cys-loop superfamily of ligand-gated ion channels. The ligand-binding domain was modelled using the X-ray crystal structure of the acetylcholine binding-protein (AChBP) of the pond snail *Lymnaea stagnalis* at a 2.7 Å resolution (PDB entry 1I9B) [16]. Although this soluble protein is not part of the Cys-loop superfamily, it bears 15–24% sequence identity with the LBD of this group of proteins, and has a similar fold to the LBD of Cys-loop proteins. Each of the five subunits which form the AChBP pentamer are comprised of one N-terminal α-helix, two short 3_{10} helices and a large β-sandwich consisting of 10 β-strands [16] (it should be noted that a model of the complete nAChR of *T. marmorata* based on cryo-electron microscopy studies has recently been published [6]).

2.2. Sequence alignment

Proper sequence alignment between template and target structures is a critical step in building a useful comparative or homology model. The slightest misalignment may yield models with little validity. The task is further complicated when dealing with low-homology sequences, as in the present

case. Moreover, insertions and deletions of short segments are to be expected, as they often contribute to specificity among proteins of a given superfamily.

A multiple sequence alignment was conducted on 40 sequences, including the templates and targets, as well as other homologous protein subunits. Sequences used in the multiple sequence alignment were chosen following a series of BLAST queries performed using the Swiss Institute of Bioinformatics BLAST Network service (http://www.expasy.org/tools/blast/), which uses the NCBI BLAST 2 software [17], to identify high similarity sequences with each of the target (human $GABA_A$ α_1, β_2 and γ_2 subunits) and template (*T. marmorata* nAChR α, β, γ and δ subunits, and *L. stagnalis* AChBP) mature sequences. Multiple sequence alignment aids in obtaining meaningful alignments, especially in regions of low similarity between template and target sequences, by including information on other related sequences which may have higher similarity with one or both of these sequences. All sequences identified belonged to the Cys-loop superfamily of ligand-gated ion channels, except for the AChBP template. A subset of 40 sequences was chosen to limit the bias towards certain proteins or subunit isoforms. The multiple sequence alignment was performed with the Molecular Operating Environment (MOE) program [18], using the PAM250 substitution matrix. The sequence alignment is shown in Fig. 2 for the TMD of the three subunit target sequences ($GABA_A$ α_1, β_2 and γ_2) and the four template sequences used in modelling the TMD (nAChR α, β, γ and δ).

2.3. Subunit assignment

Assigning subunit correspondence between the nAChR and $GABA_A$ subunits is straightforward due to the functional homology between members of the cys-loop superfamily. The ACh binding pockets of the nAChR are located at the α(+)/γ(−) and α(+)/δ(−) subunit interfaces of the LBD, whereas the homologous GABA binding pockets of $GABA_A$ are situated at the two β(+)/α(−) subunit interfaces. The $GABA_A$ β subunits were thus assigned to the nAChR α subunits, and the remaining subunits were assigned accordingly (Fig. 1b).

2.4. Mapping sequence onto structure

All steps of the model building and refinement were conducted with Sybyl versions 7.0 and 7.1 [19] on an Octane SGI station, unless stated otherwise. The target sequences were mapped onto the appropriate template subunits, omitting loop segments, according to the multiple sequence alignment obtained above. By maintaining torsion angles from the templates, secondary structure was preserved, hence allowing for fold conservation.

2.5. Refinement of the TMD

One of the main objectives in constructing a molecular model of the $GABA_A$ channel was to provide a model that was compatible with known experimental data concerning the binding and action of general anaesthetics at this receptor. Consequently, particular consideration was given to the description of the region known to be implicated in general anaesthetic action. Experimental evidence has shown that residues in a binding pocket located at the centre of the four transmembrane α-helices composing the TMD of subunits such as α_1 and β_2 are involved in binding various general anaesthetics. Hydrophobicity profiles of the TMD α-helices were generated based on the Kyte–Doolittle hydrophobicity scale for amino acids (Table 1) [20]. This scale was used, together with available experimental data, to determine appropriate rotations of segments which did not account for all experimental data. This will be further discussed in Section 3.

A second refinement step was required because of an inconsistency between the two templates being used. The cryo-electron microscopy structure of the nAChR TMD represents the closed-pore state of the ion channel [5], while the X-ray

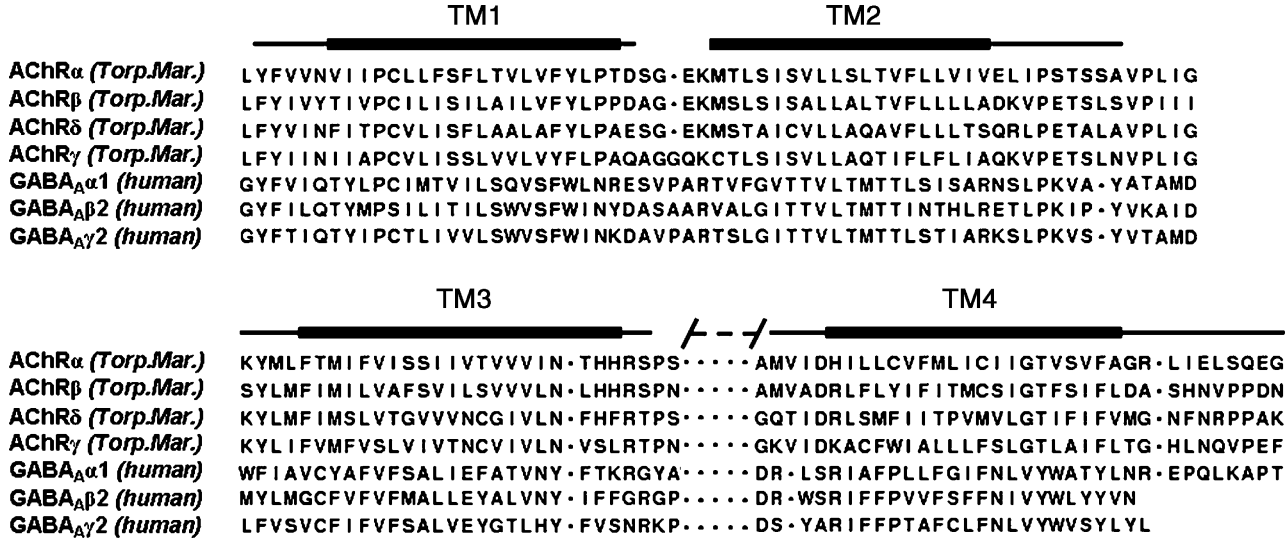

Fig. 2. Multiple sequence alignment of the TMD (except for the long TM3–TM4 loop) of all four template sequences (nAChR α, β, δ, and γ) and target sequences ($GABA_A$ α, β, and γ). The lines above the alignment indicate the α-helices, with the transmembrane segments indicated with bold lines.

Table 1
Kyte–Doolittle hydrophobicity scale

Amino acid	Hydrophobicity
Ala	1.8
Arg	−4.5
Asn	−3.5
Asp	−3.5
Cys	2.5
Gln	−3.5
Glu	−3.5
Gly	−0.4
His	−3.2
Ile	4.5
Leu	3.8
Lys	−3.9
Met	1.9
Phe	2.8
Pro	−1.6
Ser	−0.8
Thr	−0.7
Trp	−0.9
Tyr	−1.3
Val	4.2

crystal structure of the AChBP used as a template for the LBD is in the ligand-bound, open-pore state [16]. For the nAChR, the open-pore structure of the LBD differs from that of the closed-pore by a small conformational adjustment in the ACh binding pocket caused by ligand binding, and by larger conformational alterations, mainly at the level of the nAChR α subunits [21,22]. In the nAChR unbound state, the inner β-sheets of the α subunits are rotated by an anticlockwise rotation of approximately 15–16°, while the inner β-sheets of the other subunits are modified by less than 2°. Furthermore, the outer β-sheets are tilted, by 13–16° for the α subunits and less than 5° for the other subunits [21,22]. The rotations sustained by the LBD subunits upon binding of ACh, mainly in the α subunits, are propagated to the TMD. Within the LBD, the open-pore is pseudo-symmetrical, while the closed-pore is asymmetrical, with the α subunits in a conformation distinct from that of the other subunits. Hence, since the LBD template (AChBP) represents the open-state of the ion channel and the TMD template (nAChR) represents the closed-state, modification of one domain was required to create a consistent model.

Since one of the main objectives was to generate a model compatible with known data concerning general anaesthetic binding, the open-state channel was ultimately selected. Bormann et al. demonstrated that the ion pore of the open $GABA_A$ channel should have, at its narrowest dimension, a diameter of 5–6 Å [4]. However little is known concerning how the structure of the TMD is altered upon allosteric modulation via the LBD. A homologous rotation or twisting motion in all TM2 α-helices, independent of subunit identity, has been proposed, although this has not been confirmed due to the low-medium resolution of current nAChR structures [21,23]. Nevertheless, it is most likely that the conformational changes in the LBD are conveyed to the TM2 segments via interactions between the TM2–TM3 loop and the L2 and L7 loops, causing the TM2 helices to move outwards, towards the surrounding TM1, TM3 and TM4 helices, hence widening the ion pore [2,5,6,22,24]. The motions in TM1, TM3 and TM4 are estimated to be much more subtle since they are surrounded by the membrane bilayer. The pore was thus widened by fixing the relative geometry of all TM1, TM3 and TM4 segments, and moving each TM2 segment away from the centre of the TMD (which lies on the five-fold axis) towards the centre of their respective subunits. First, a 0.5 Å displacement of the TM2 helices was investigated. However upon minimization of the model, this did not yield an adequate pore width and thus a 1.0 Å displacement was used instead. Prior to minimization, side chain torsion angles were scanned to remove steric clashes. Sybyl uses a rotamer library to find more favourable side chain conformations which alleviate such steric overlap.

2.6. Loop modelling

We define loops as segments in the sequence alignment of low similarity which differ in length due to insertions or deletions in the primary sequence. Two methods were investigated in modelling loops of the $GABA_A$ model, as described below.

The first approach involved searching a database of loops available within the Sybyl7.0 package [19]. A search allows the identification of loops that possess the same number of residues as the target loop, and that minimize the RMSD of the anchor residues connecting the loop to the rest of the protein structure. Additional criteria are then used to select which of these loops is believed to provide the best loop structure. The criteria considered were as follows: (1) maximizing sequence homology with the target loop, (2) minimizing unfavourable steric contacts with the remainder of the protein, and (3) other criteria based on available experimental data. The main advantage of database loop searching is that it is very time efficient and can often give reasonable starting structures. However, several disadvantages can be noted. First, it does not actually search conformational space and is therefore limited by the loops included in the database. Secondly, it ignores the identity of the amino acid sequence, which is particularly significant when it includes proline residues.

To overcome some of these problems, we devised an alternative approach to loop modelling – the ‘‘quasi-*ab initio* loop modelling approach’’. Quasi-*ab initio* loop modelling is based on an algorithm that generates potential loop candidates from sequence information and structural data, rather than selecting loops from pre-existent collections of loop structures. Ideally, the entire conformational space should be searched for each loop being modelled. However, a systematic search is not feasible even for relatively small loops. Consequently, a random search may be more appropriate due to the inherently large size of the conformational space. To make this search more efficient than a random search, available structural data for each individual amino acid are used. We refer to this biased random search as quasi-*ab initio*, since it uses the primary sequence of the loop as well as additional structural data.

The algorithm developed generates potential loop candidates by selecting torsion angles for individual amino acids according

to the loop's primary sequence from trivariate gaussian probability functions developed by Cheng et al. [25]. These trivariate gaussian probability functions reflect experimental values for the φ, ψ, and χ^1 torsions of amino acids found in the PDB. There exist 12 different conformational states for each amino acid, but only 4 for glycine, alanine and proline. In their work, Cheng et al. demonstrated that their trivariate gaussian probability functions could allow exploration of the conformational space for short sequences [25]. Accordingly, it was reasoned that using these trivariate gaussian probability functions could enable a size reduction of the conformational space to be explored. As loops are generated, they are analyzed to identify loops that minimize the RMSD of the anchor residues connecting the loop to the rest of the protein structure. This approach was implemented with MATLAB 6 [26]. The selected loop candidates were then further examined to pinpoint loops that minimized unfavourable steric contacts with themselves as well as with the rest of the protein, and satisfied other criteria based on available experimental data, such as the relative position of particular residues thought to be involved in the GABA binding pocket.

Selected loops were connected to the corresponding anchor residues, and were conformationally optimized via energy minimization calculations within their protein environment, using the Tripos force field [27] and a conjugate gradient energy minimization algorithm. The loop residues as well as two residues on either side of the anchor residues were geometry optimized, while the rest of the protein was constrained. The Tripos force field was used to perform the local energy minimizations since the parameters used in the loop-modelling algorithm reflect those of the Tripos force field. Loop modelling was performed on the LBD before merging with the TMD, while the TMD was refined, geometry optimized, and merged with the LBD before loop modelling was performed. This was especially important for the TM2–TM3 loop, as it interacts with the L2 and L7 loops in the respective subunit LBDs.

2.7. Model assembly

The LBD (after loop modelling) and TMD (after refinement but before loop modelling) were initially geometry optimized individually by performing an energy minimization using the Amber4.1 charges and force field [28] with an initial 200 steps of Simplex minimization followed by 1000 steps of steepest descent minimization. They were then merged by overlapping their five-fold pore-traversing axes and aligning the corresponding subunits, minimizing the distance between connecting residues. Next, quasi-*ab initio* loop modelling was carried out on the TMD loops, as well as for the connecting segments (five residues long) between the LBD and TMD sections of each subunit. Side-chain torsion angles were scanned to identify corrections that alleviated unfavourable steric interactions. The assembled model was finally geometry optimized by performing an initial 200 steps of Simplex minimization followed by a steepest descent minimization to reach a root-mean-square (RMS) force of 1.0 kcal/mol/Å, and subsequently a conjugate gradient minimization to reach a RMS force of 0.5 kcal/mol/Å.

3. Results

3.1. Dimensions of the model

The complete assembled and energy minimized $GABA_A$ model (Fig. 3, generated using the ArgusLab program [29]) has

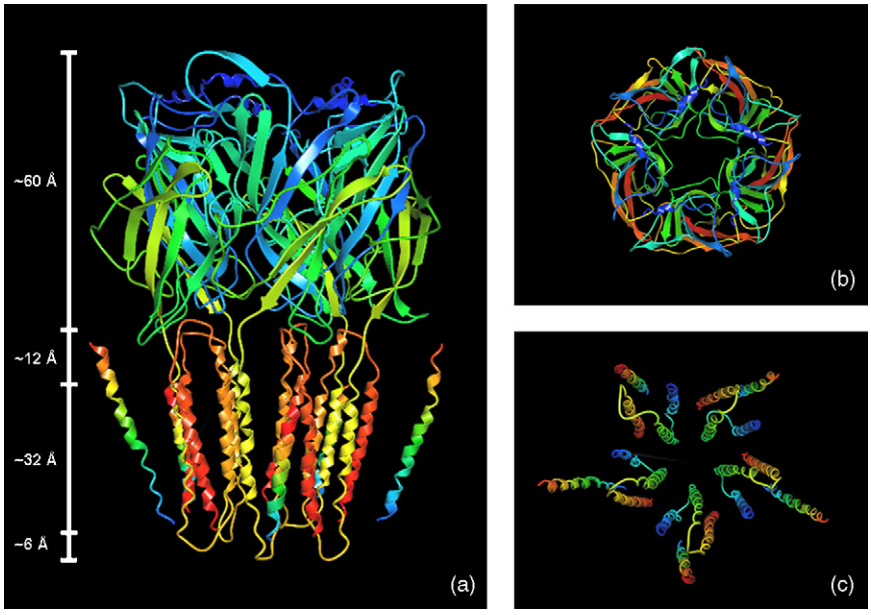

Fig. 3. (a) Side view of the $GABA_A$ model; the TMD (bottom) spans through the lipid membrane (~32 Å) and partly on the extracellular side (~12 Å), while the LBD (top) is completely extracellular (~60 Å). (b) The LBD viewed from the extracellular side (diameter of ~80 Å). (c) The TMD viewed from the extracellular side. Arrows and ribbons (which correspond to β-strands and α-helices, respectively) are coloured according to position in each individual subunit sequence, as well as in the TM4 of each subunit which is not bonded to the rest of the model. It should be noted that the colour scheme is thus different in all three pictures. In (b) and (c), this clearly allows differentiation between all five subunits.

a total length of ~110 Å along the five-fold axis, and a maximum width of ~80 Å perpendicular to the five-fold axis. The ion pore is, at its widest, ~18 Å in diameter, and at its narrowest, ~6 Å. This model represents the open-pore structure of the $GABA_A$ channel. The LBD measures ~60 Å along the five-fold axis, while the TMD measures ~50 Å. The TMD is expected to span ~12 Å beyond the lipid bilayer on the extracellular side of the membrane and ~6 Å on the cytoplasmic side. This omits the cytoplasmic domain, which was not included in the model since little is known about its secondary structure, although it has recently been proposed that it includes a curved α-helix which precedes TM4 [6].

3.2. The general anaesthetic binding site

An initial model of the TMD was constructed without conducting structural refinements based on hydrophobicity profiles. In this first model, the relative orientation of the TMD α-helices was determined solely on the sequence alignment shown in Fig. 2. However, there is uncertainty in the sequence alignment of the TMD due to low sequence similarity, particularly in the cases of TM3 and TM4. Different alignments have been proposed in the literature, but it remains unclear which alignment provides a more accurate model. For example, our alignment (Fig. 2) differs from that published by Ernst et al. [30] for TM3 and TM4, but agrees with the alignment suggested by Bertaccini et al. [31].

The alignment is also supported by the observation by Miyazawa et al. that there are negatively charged and polar residues near the membrane-extracellular and membrane-cytoplasm interfaces in the TM1 (α-Asn217 and α-Asp238), TM2 (α-Glu241 and α-Glu262) and TM4 (α-Asp407 and α-Gly428) segments of the nAChR electron microscopy structure [5]. In our sequence alignment (Fig. 2), we also note the presence of positively charged residues near the membrane-cytoplasm interface in the TM2 (nAChR α-Lys242) and TM4 (nAChR α-His408) segments. These are most likely conserved due to the specific nature of the interactions, and our alignment involves similar residues at these interface positions. Although considered, an alignment shift was thus excluded due to the presence of these conserved polar and charged residues. By rotating the α-helices rather than shifting the alignment, these polar and charged residues remain at the membrane interfaces. It should however be noted that the alignment of the TM3 segment includes more ambiguity and an alignment shift may lead to a more representative structure. For example, in the alignment proposed by Ernst et al. [30] the TM3 sequence alignment is shifted by one residue when compared to our alignment, placing the $GABA_A$ α_1-Ala291 (thought to be involved in the volatile anaesthetic binding pocket) at the TM3–TM4 interface rather than towards the lipid membrane when mapped onto the nAChR template. Refinement of the TMD is further justified since the template used (nAChR) was obtained at a 4 Å resolution.

In an attempt to validate this procedure, the hydrophobicity profiles were repeated for the *T. marmorata* nAChR TMD. Similar profiles were obtained for both the $GABA_A$ and nAChR transmembrane sequences, however differences in the hydrophobicity of windows around the transmembrane segments were less pronounced for the nAChR. The transmembrane portions of the nAChR TM1 and TM4 helices had a more uniform hydrophobicity profile compared to the corresponding $GABA_A$ segments, whereas the TM3 segments had rather uniform hydrophobicity profiles for both the nAChR and $GABA_A$ sequences, indicating that the approach may be less suitable for the TM3 segment than for the TM1 and TM4 segments.

The computational model of the $GABA_A$ channel being developed in this study endeavours to provide a model compatible with known experimental data concerning binding and action of general anaesthetics, which bind in a pocket situated between the four α-helices forming the TMD of specific subunit isoforms. In the α_1 subunit, residues Leu232 (TM1), Ser270 (TM2) and Ala291 (TM3) have been shown to be involved in alcohol and volatile anaesthetics binding, as have the homologous β_2 subunit residues Asn265 (TM2) and M286 (TM3) [32–37]. Moreover, tryptophan scanning mutagenesis studies of the TM4 segment of the α_1 subunit show that three additional residues may also be involved in the alcohol and volatile anaesthetic binding pocket, namely Tyr411, Thr414 and Tyr415 [38]. In the β_2 subunit, Asn265 (TM2) has likewise been shown to play a role in modulation by etomidate [15,32], while Met286 (TM3) has been shown to be involved in a binding pocket for propofol and related alkylphenols [32,39]. Upon inspection of our initial model of the TMD, only the Ser270 residue (TM2), involved in the alcohol and volatile anaesthetic binding pocket of the α_1 subunit, was located within this inter-α-helical pocket (as well as the homologous residues in the other subunits, including Asn265 in the β_2 subunit), whereas Leu232, Ala291 and the potential Tyr411, Thr414 and Tyr415 residues were not. Moreover, the pore-lining α_1 residues Val257, Thr261, Leu264, Thr265 and Thr268 [1,40] (and the equivalent residues for the β_2 and γ_2 subunits) were correctly positioned towards the lumen of the ion pore. Hence, the TM2 helix was maintained in its original orientation while further investigation was deemed necessary for TM1, TM3 and TM4.

The TMD α-helices of the α_1, β_2 and γ_2 subunits were analyzed to determine their hydrophobicity profiles. The average hydrophobicity of the α-helices along each possible face was computed using the Kyte–Doolittle hydrophobicity scores for amino acids (Table 1) [20]. Only segments of the α-helices predicted to be located within the lipid membrane were used in calculating hydrophobicity profiles. These segments, shown in Fig. 2, correspond to the transmembrane regions identified in the cryo-electron microscopy structure of the *T. marmorata* nAChR [5]. Hydrophobicity scores were calculated at increments of 20° around the main axis of the α-helices, with a window width of 80° (this corresponds to a window spanning ±40° from the relative angle reported on the *X*-axis in Fig. 4a–d). This width was chosen since it represents the approximate window accessible to the lipid bilayer (TM1 and TM3), the ion pore (TM2) or the inter-α-helical pocket (TM4). Hydrophobicity scores for each window were computed by averaging the

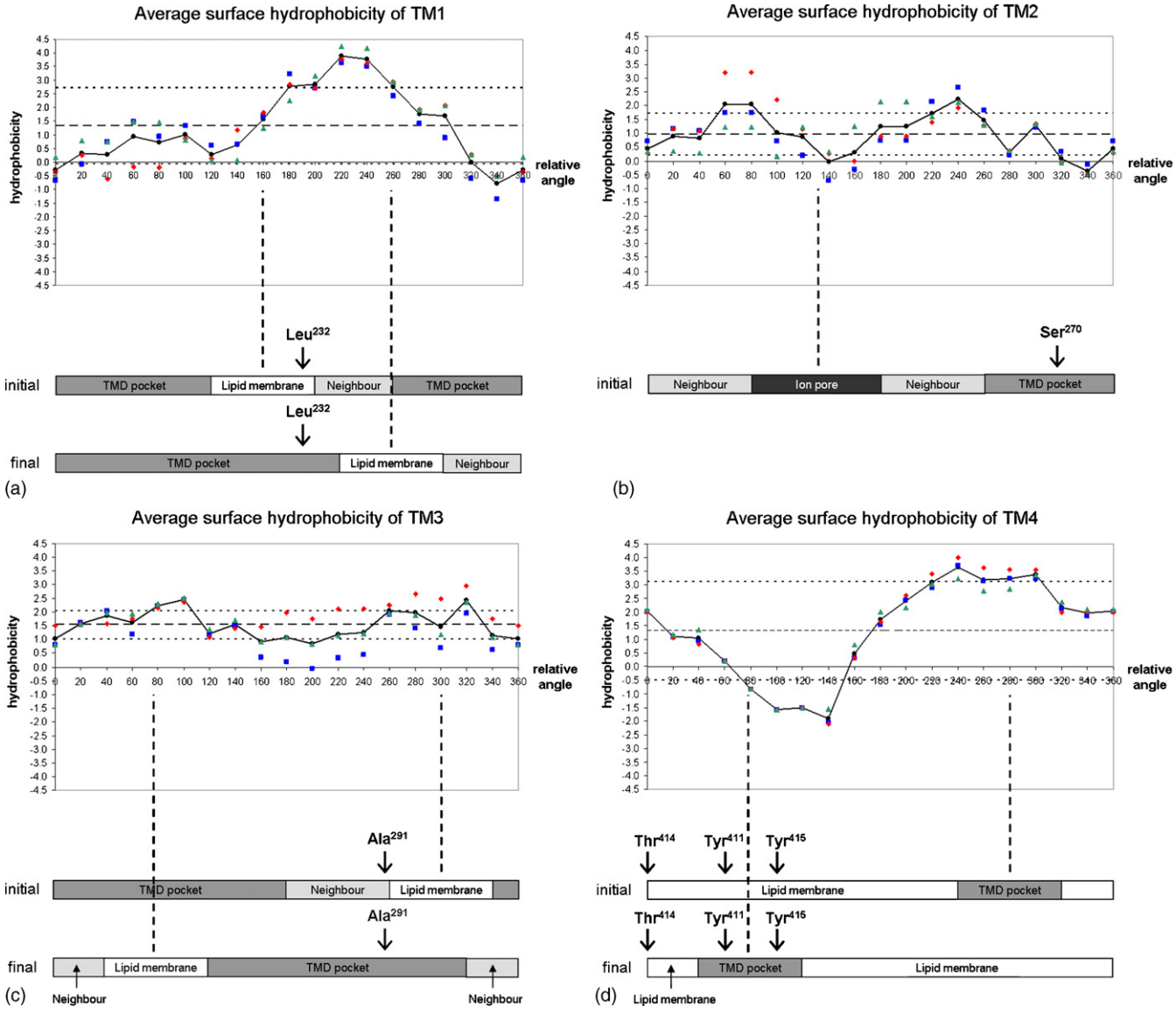

Fig. 4. Average surface hydrophobicity plots for (a) TM1, (b) TM2, (c) TM3, and (d) TM4. Hydrophobicity of the α_1 (■), β_2 (◆), and γ_2 (▲) subunits are presented, as well as the average hydrophobicity for all three subunits (–●–). The middle dashed line indicates the average window hydrophobicity of a given TMD α-helix, while two other dashed lines are placed one standard deviation above and below the average window hydrophobicity. Below the plots, diagrams present the initial and final positions of the α-helices with respect to their environment, with key residues indicated by arrows.

individual amino acid hydrophobicity scores of all amino acids along the length of the α-helix within a given window. The hydrophobicity profiles obtained are shown in Fig. 4.

Optimal orientations of the TM1 and TM3 helices were defined as those for which the hydrophobicity of the lipid-facing window exceeded the average window hydrophobicity for the given TM segment by more than one standard deviation. This corresponds to a relative angle between 180° and 260° for TM1 (Fig. 4a), and a relative angle of 80°, 100° or 320° for TM3 (Fig. 4c). Rotations for TM1 and TM3 (to 260° and 80°, respectively) were chosen to maximize the hydrophobicity of the lipid-accessible face while allowing for residues involved in the anaesthetic binding pocket to be positioned within the inter-α-helical pocket, as shown at the bottom of Figs. 4a and 4c. Optimal orientations of the TM4 helix were defined as those for which the hydrophobicity of the non-lipid-facing window was more than one standard deviation below the average window hydrophobicity score for TM4. This was between 80° and 140°, and a rotation to 80° was chosen to position Tyr411 and Tyr415 in the inter-α-helical pocket. The potentially involved Thr414 residue could not be positioned within the pocket due to the helical nature of the TM4 segment. The resulting volatile anaesthetic binding pocket found in the α_1 subunit is shown in Fig. 5.

3.3. The GABA binding site

Other regions of interest in the $GABA_A$ model include the GABA binding sites, which are located at the β(+)/α(−) interfaces. According to experimental data, the GABA binding pocket is lined by various residues including Phe65, Arg67, Ser69, Arg120, Ile121, Arg177, Val179, Val181 and Asp184

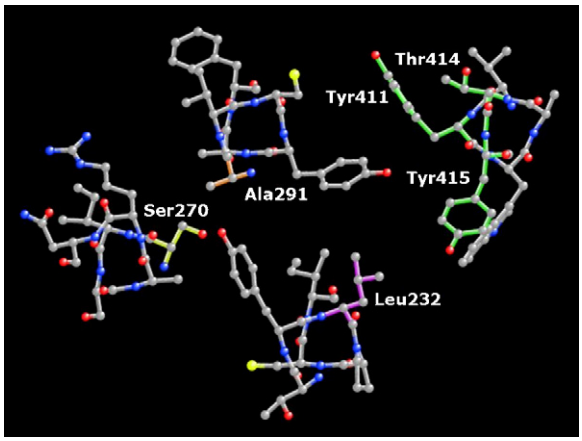

Fig. 5. Illustration of the volatile anaesthetic binding pocket of the α_1 subunit (Leu232: pink; Ser270: yellow; Ala291: orange; Tyr411, Thr414 and Tyr415: green).

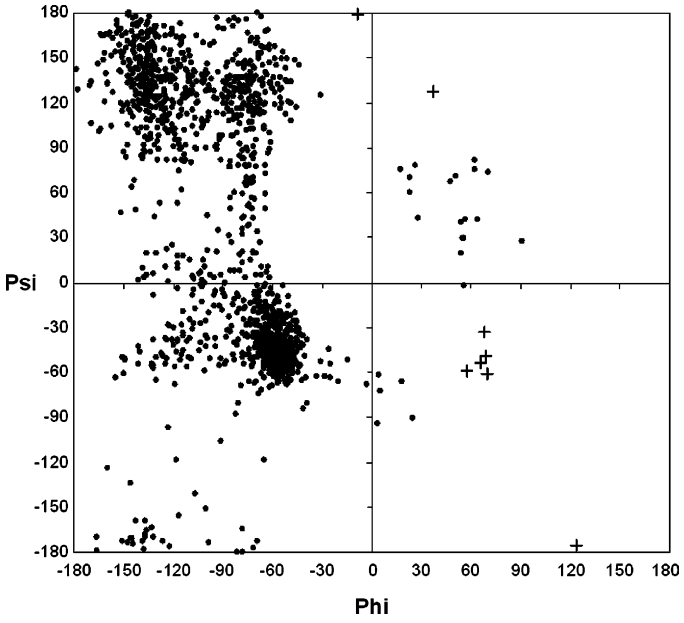

Fig. 6. Ramachandran plot of all residues (allowed: •; disallowed: +), except for proline and glycine residues which have different typical Ramachandran plots.

from the α_1 subunit, and Tyr97, Leu99, Tyr157, Thr160, Thr202, Ser204, Tyr205, Arg207 and Ser209 from the β_2 subunit [41–48]. Six of these amino acids are in loops in which the sequence alignment (see supplementary data) demonstrates that the $GABA_A$ subunits have a different number of amino acids with respect to the AChBP template. These residues correspond to Arg177, Val179, Val181 and Asp184 from the L9 loop of the α_1 subunit, and residues Thr202 and Ser204 from the L10 loop of the β_2 subunit. These two loops were modelled using the quasi-*ab initio* loop modelling approach.

The loops chosen accounted for all available experimental evidence, placing the above mentioned residues (α_1: Arg177, Val179, Val181 and Asp184; β_2: Thr202 and Ser204) within a putative GABA binding pocket. Although it is argued that this provides an appropriate guess, until the experimental structure of the $GABA_A$ channel can be elucidated, it is not possible to know how well this model truly describes the GABA binding pocket. In fact, it is undoubtedly one of the most uncertain regions since it is delimited, amongst others, by two loops which were modelled with the quasi-*ab initio* loop modelling algorithm. Furthermore, the L9 loop of the α_1 subunit was modelled using a 12 residue long segment, and it is known that both *ab initio* and knowledge-based methods do poorly for loops longer than 7–8 residues long.

3.4. Coupling of the LBD and TMD

Several regions are implicated in coupling agonist binding in the LBD with channel gating in the TMD. As previously mentioned, conformational changes in the LBD are conveyed to the TM2 segments through interactions between the L2 and L7 loops of the LBD and the TM2–TM3 loop [2,5,6,22,24]. More specifically, it has been proposed that electrostatic interactions between Asp57 and Asp149, from loops L2 and L7, respectively, and Lys279 from TM2–TM3, may play a role in channel gating in the α_1 subunits [24]. Homologous residues were identified in the β_2 subunit, however it was noted that charge reversal double mutants did not restore receptor function, whereas they did for the α_1 subunits [24,49]. In our model, the TM2–TM3 loop intercalates between L2 and L7, as is also observed in the recently published cryo-electron microscopy structure of nAChR [6]. However, the charged residues on these loops do not appear to be in close proximity, and no electrostatic interaction is noted between them. Another pair of charged residues on the β_2 subunit, namely Asp146 in loop L7 and Lys215 in the pre-TM1 segment, has been found to be in close proximity in the GABA-bound receptor [49]. In our model, these residues are located 1.6–1.7 Å apart in the two β_2 subunits.

3.5. Overall stereochemical quality

Beyond ensuring that most available experimental criteria were satisfied, additional validation tests were conducted using the MOE software [18], to assess the model's stereochemical quality. The protein report generated by MOE indicated that all but eight residues had phi and psi dihedral angles which fell within the accepted regions of the Ramachandran plot (Fig. 6). Among the pairs of non-bonded atoms, 47 were identified as having their van der Waals radii overlap by more than the default value of 70%, which corresponded in all cases to interatomic distances greater than 2.3 Å. All bond angles, bond lengths and C_α chirality were found to be adequate. Overall, the structure was deemed satisfactory.

4. Discussion

Although experimental evidence has previously demonstrated the involvement in general anaesthetic binding of various residues located at the centre of the four α-helices composing the TMD of specific $GABA_A$ subunit isoforms at one or multiple closely positioned sites, the exact 3D arrangement of these residues within the binding site and the precise interactions with putative general anaesthetics remain

unclear. The first step in establishing a potential geometry and environment of this binding pocket was therefore to develop a model of the $GABA_A$ receptor. Modelling of the TMD was complicated by two main factors. First, the template used, namely the cryo-electron microscopy structure of the *T. marmorata* nAChR TMD, was obtained at a low-medium resolution of 4 Å [5]. Secondly, there exists low sequence homology between the $GABA_A$ and nAChR TMD α-helices, especially between the TM3 and TM4 segments, and, to a lesser extent, between the TM1 segments (Fig. 2).

Our refinement procedure generated a model that places the residues involved in general anaesthetic binding within this inter-α-helical pocket while respecting hydrophobicity constraints of the protein and lipid membrane environment. Unfortunately, until a high resolution structure of the $GABA_A$ channel can be elucidated, little can be done to verify to what extent this model is representative of the actual binding site. Nevertheless, it presents a model that respects both the hydrophobicity constraints of the TMD's environment and most available experimental data. It thus provides a reasonable initial model that can be exploited in the design of future experimental studies. Furthermore, as new experimental data become available for the $GABA_A$ protein and other members of the Cys-loop superfamily, this will enhance our capability of further refining the current model and generating more accurate models of the $GABA_A$ channel.

5. Conclusion

A computational model of the $\alpha_1\beta_2\gamma_2$ $GABA_A$ ligand-gated ion channel was built using a comparative modelling approach. The nAChR TMD from *T. marmorata* [5] and the AChBP from *L. stagnalis* [16] were used as templates to model the TMD and LBD, respectively, and loop modelling as well as refinement procedures including hydrophobicity profiling of the transmembrane α-helices were conducted so as to yield a model satisfying most available experimental data concerning general anaesthetic binding.

Acknowledgements

VC-S acknowledges salary support from the Natural Science and Engineering Research Council of Canada and the Killam Trust. DFW is a Canada Research Chair, Tier I, in neuroscience. This research was supported by operating grants from the Natural Science and Engineering Research Council of Canada and the Atlantic Innovation Fund.

Appendix A. Supplementary data

Supplementary data associated with this article can be found, in the online version, at doi:10.1016/j.jmgm.2006.06.001.

References

[1] A. Karlin, Emerging structure of the nicotinic acetylcholine receptors, Nat. Rev. Neurosci. 3 (2002) 102–114.
[2] T.L. Kash, J.R. Trudell, N.L. Harrison, Structural elements involved in activation of the γ-aminobutyric acid type A ($GABA_A$) receptor, Biochem. Soc. Trans. 32 (3) (2004) 540–546.
[3] M.L. Jensen, A. Schousboe, P.K. Ahring, Charge selectivity of the Cys-loop family of ligand-gated ion channels, J. Neurochem. 92 (2005) 217–225.
[4] J. Bormann, O.P. Hamill, B. Sakmann, Mechanism of anion permeation through channels gated by glycine and γ-aminobutyric acid in mouse cultured spinal neurones, J. Physiol. (Lond.) 385 (1987) 243–286.
[5] A. Miyazawa, Y. Fujiyoshi, N. Unwin, Structure and gating mechanism of the acetylcholine receptor pore, Nature 423 (6943) (2003) 949–955.
[6] N. Unwin, Refined structure of the nicotinic acetylcholine receptor at 4 Å resolution, J. Mol. Biol. 346 (2005) 967–989.
[7] P. Krogsgaard-Larsen, B. Frølund, T. Liljefors, Specific $GABA_A$ agonists and partial aonists, Chem. Rec. 2 (2002) 419–430.
[8] M. Chebib, G.A.R. Johnston, GABA-activated ligand gated ion channels: medicinal chemistry and molecular biology, J. Med. Chem. 43 (8) (2000) 1427–1447.
[9] E. Sigel, A. Buhr, The benzodiazepine binding site of $GABA_A$ receptors, Trends Pharmacol. Sci. 18 (1997) 425–429.
[10] A. Buhr, R. Baur, E. Sigel, Subtle changes in residue 77 of the subunit of $\alpha1\beta2\gamma2$ $GABA_A$ receptors drastically alter the affinity for ligands of the benzodiazepine binding site, J. Biol. Chem. 272 (18) (1997) 11799–11804.
[11] A. Buhr, E. Sigel, A point mutation in the γ2 subunit of γ-aminobutyric acid type A receptors results in altered benzodiazepine binding site specificity, Proc. Natl. Acad. Sci. U.S.A. 94 (16) (1997) 8824–8829.
[12] R.M. McKernan, S. Farrar, I. Collins, F. Emms, A. Asuni, K. Quirk, H. Broughton, Photoaffinity labeling of the benzodiazepine binding site of $\alpha1\beta3\gamma2$ γ-aminobutyric $acid_A$ receptors with flunitrazepam identifies a subset of ligands that interact directly with His102 of the α subunit and predicts orientation of these within the benzodiazepine pharmacophore, Mol. Pharmacol. 54 (1998) 33–43.
[13] K.A. Wafford, $GABA_A$ receptor subtypes: any clue to the mechanism of benzodiazepine dependence? Curr. Opin. Pharmacol. 5 (2005) 47–52.
[14] C. Hill-Venning, D. Belelli, J.A. Peters, J.J. Lambert, Subunit-dependent interaction of the general anaesthetic etomidate with the γ-aminobutyric acid type A receptor, Br. J. Pharmacol. 120 (1997) 749–756.
[15] D. Belelli, J.J. Lambert, J.A. Peters, K.A. Wafford, P.J. Whiting, The interaction of the general anesthetic etomidate with the γ-aminobutyric acid type A receptor is influenced by a single amino acid, Proc. Natl. Acad. Sci. U.S.A. 94 (1997) 11031–11036.
[16] K. Brejc, W.J. van Dijk, R.V. Klaassen, M. Schuurmans, J. van der Oost, A.B. Smit, T.K. Sixma, Crystal structure of an ACh-binding protein reveals the ligand-binding domain of nicotinic receptors, Nature 411 (6835) (2001) 269–276.
[17] S.F. Altschul, T.L. Madden, A.A. Schäffer, J. Zhang, Z. Zhang, W. Miller, D.J. Lipman, Gapped BLAST and PSI-BLAST: a new generation of protein database search programs, Nucleic Acids Res. 25 (1997) 3389–3402.
[18] MOE Program, Chemical Computing Group Inc., Montréal, Québec, Canada, 2003.
[19] SYBYL, version 7.1, Tripos Inc., 1699 South Hanley Road, St. Louis, MI 63144, USA, 2005.
[20] J. Kyte, R. Doolittle, A simple method for displaying the hydropathic character of a protein, J. Mol. Biol. 157 (1982) 105–132.
[21] N. Unwin, Structure and action of the nicotinic acetylcholine receptor explored by electron microscopy, FEBS Lett. 555 (2003) 91–95.
[22] N. Unwin, A. Miyazawa, J. Li, Y. Fujiyoshi, Activation of the nicotinic acetylcholine receptor involves a switch in conformation of the α subunits, J. Mol. Biol. 319 (2002) 1165–1176.
[23] C. Bouzat, F. Gumilar, G. Spitzmaul, H.-L. Wang, D. Rayes, S.B. Hansen, P. Taylor, S.M. Sine, Coupling of agonist binding to channel gating in an ACh-binding protein linked to an ion channel, Nature 430 (2004) 896–900.
[24] T.L. Kash, A. Jenkins, J.C. Kelley, J.R. Trudell, N.L. Harrison, Coupling of agonist binding to channel gating in the $GABA_A$ receptor, Nature 421 (2003) 272–275.

[25] B. Cheng, A. Nayeem, H.A. Scheraga, From secondary structure to three-dimensional structure: improved dihedral angle probability distribution function for use with energy searches for native structures of polypeptides and proteins, J. Comput. Chem. 17 (12) (1996) 1453–1480.
[26] MATLAB, version 6.0.0.88 Release 12, The MathWorks Inc., Massachusetts, USA, 2000.
[27] M. Clark, R.D. Cramer III, N. van Opdenhosch, Validation of the general purpose tripos 5.2 force field, J. Comput. Chem. 10 (1989) 982–1012.
[28] W.D. Cornell, P. Cieplak, C.I. Bayly, I.R. Gould, K.M.J. Merz, D.M. Ferguson, D.C. Spellmeyer, T. Fox, J.W. Caldwell, P.A. Kollman, A second generation force field for the simulation of proteins, nucleic acids and organic molecules, J. Am. Chem. Soc. 117 (1995) 5179–5197.
[29] ArgusLab, version 4.0.1, Mark Thompson and Planaria Software LLC, Seattle, USA, 2004.
[30] M. Ernst, S. Bruckner, S. Boresch, W. Sieghart, Comparative models of $GABA_A$ receptor extracellular and transmembrane domains: important insights in pharmacology and function, Mol. Pharmacol. 68 (5) (2005) 1291–1300.
[31] E.J. Bertaccini, J. Shapiro, D.L. Brutlag, J.R. Trudell, Homology modeling of a human glycine alpha 1 receptor reveals a plausible anesthetic binding Site, J. Chem. Inf. Model. 45 (1) (2005) 128–135.
[32] M.D. Krasowski, N.L. Harrison, General anaesthetic actions on ligand-gated ion channels, Cell. Mol. Life Sci. 55 (1999) 1278–1303.
[33] J.R. Trudell, E. Bertaccini, Comparative modeling of a GABAA alpha1 receptor using three crystal structures as templates, J. Mol. Graphics Modell. 23 (2004) 39–49.
[34] S. Ueno, A. Lin, N. Nikolaeva, J.R. Trudell, S.J. Mihic, R.A. Harris, N.L. Harrison, Tryptophan scanning mutagenesis in TM2 of the $GABA_A$ receptor α subunit: effects on channel gating and regulation by ethanol, Br. J. Pharmacol. 131 (2) (2000) 296–302.
[35] A. Jenkins, E.P. Greenblatt, H.J. Faulkner, E. Bertaccini, A. Light, A. Lin, A. Andreasen, A. Viner, J.R. Trudell, N.L. Harrison, Evidence for a common binding cavity for three general anesthetics within the $GABA_A$ receptor, J. Neurosci. 21 (RC136) (2001) 131–134.
[36] M.P. Mascia, J.R. Trudell, R.A. Harris, Specific binding sites for alcohols and anesthetics on ligand-gated ion channels, Proc. Natl. Acad. Sci. U.S.A. 97 (16) (2000) 9305–9310.
[37] S.J. Mihic, Q. Ye, M.J. Wick, V.V. Koltchine, M.D. Krasowski, S.E. Finn, M.P. Mascia, C.F. Valenzuela, K.K. Hanson, E.P. Greenblatt, R.A. Harris, N.L. Harrison, Sites of alcohol and volatile anaesthetic action on GABAA and glycine receptors, Nature 389 (1997) 385–389.
[38] A. Jenkins, A. Andreasen, J.R. Trudell, N.L. Harrison, Tryptophan scanning mutagenesis in TM4 of the $GABA_A$ receptor α1 subunit: implications for modulation by inhaled anesthetics and ion channel structure, Neuropharmacology 43 (2002) 669–678.
[39] M.D. Krasowski, K. Nishikawa, N. Nikolaeva, A. Lin, N.L. Harrison, Methionine 286 in transmembrane domain 3 of the $GABA_A$ receptor β subunit controls binding cavity for propofol and other alkylphenol general anesthetics, Neuropharmacology 41 (2001) 952–964.
[40] J. Horenstein, D.A. Wagner, C. Czajkowski, M.H. Akabas, Protein mobility and GABA-induced conformational changes in GABAA receptor pore-lining M2 segment, Nat. Neurosci. 4 (5) (2001) 477–485.
[41] S.E. Westh-Hansen, P.B. Rasmussen, S. Hastrup, J. Nabekura, K. Noguchi, N. Akaike, M.-R. Witt, M. Nielsen, Decreased agonist sensitivity of human $GABA_A$ receptors by an amino acid variant, isoleucine to valine, in the α_1 subunit, Eur. J. Pharmacol. 329 (1997) 253–257.
[42] S.E. Westh-Hansen, M.R. Witt, K. Dekermendjian, T. Liljefors, P.B. Rasmussen, M. Nielsen, Arginine residue 120 of the human $GABA_A$ receptor α_1, subunit is essential for GABA binding and chloride ion current gating, Neuroreport 10 (1999) 2417–2421.
[43] J.G. Newell, C. Czajkowski, The $GABA_A$ receptor α_1 subunit Pro^{174}-Asp^{191} segment is involved in GABA binding and channel gating, J. Biol. Chem. 278 (15) (2003) 13166–13172.
[44] A.J. Boileau, A.R. Evers, A.F. Davis, C. Czajkowski, Mapping the agonist binding site of the $GABA_A$ receptor: evidence for a β-strand, J. Neurosci. 19 (12) (1999) 4847–4854.
[45] A.J. Boileau, J.G. Newell, C. Czajkowski, $GABA_A$ receptor β_2 Tyr^{97} and Leu^{99} line the GABA-binding site, J. Biol. Chem. 277 (4) (2002) 2931–2937.
[46] G.B. Smith, R.W. Olsen, Identification of a [^{3}H]muscimol photoaffinity substrate in the bovine γ-aminobutyric $acid_A$ receptor α subunit, J. Biol. Chem. 269 (32) (1994) 20380–20387.
[47] J. Amin, D.S. Weiss, $GABA_A$ receptor needs two homologous domains of the β-subunit for activation by GABA but not by pentobarbital, Nature 366 (1993) 565–569.
[48] D.A. Wagner, C. Czajkowski, Structure and dynamics of the GABA binding pocket: a narrowing cleft that constricts during activation, J. Neurosci. 21 (1) (2001) 67–74.
[49] T.L. Kash, M.-J.F. Dizon, J.R. Trudell, N.L. Harrison, Charged residues in the β_2 subunit involved in $GABA_A$ receptor activation, J. Biol. Chem. 279 (6) (2004) 4887–4893.